Influence of Polymer Matrixes on the Photophysical Properties of UV Absorbers†

Martin Stein,‡,§ Juergen Keck,‡,|| Frank Waiblinger,‡,⊥ Anja P. Fluegge,‡ Horst E. A. Kramer,*,‡ Achim Hartschuh,# Helmut Port,# David Leppard,▽ and Gerhard Rytz▽,○

Institut für Physikalische Chemie, Universität Stuttgart, Pfaffenwaldring 55, D-70569 Stuttgart, Germany, 3. Physikalisches Institut, Universität Stuttgart, Pfaffenwaldring 57, D-70569 Stuttgart, Germany, and Ciba Specialty Chemicals, Inc., Additives Division, Rosental R 1059, CH-4002 Basle, Switzerland

Received: June 5, 2001; In Final Form: August 29, 2001

The copolymerization parameters for monomer pairs of the copolymerizable UV absorbers MA-TIN 1 (2-[2-hydroxy-3-*tert*-butyl-5-(O-[2-hydroxy-3-(2-methylpropenoyloxy)-propyl]-2-carbonyloxyethyl)phenyl]-benzotriazole) and MA-TZ 1 (2,4-bis(2,4-dimethylphenyl)-6-[2-hydroxy-4-(2-hydroxy-3-[2-methylpropenoyloxy])-propoxyphenyl]-1,3,5-triazine) with styrene and methyl methacrylate were determined. The UV absorbers were present to a higher extent in the copolymers than they are when simply present as mixtures of monomeric UV absorbers in the monomer feed. At higher temperatures, the radiationless deactivation from the excited proton-transferred singlet state becomes more efficient for the UV absorbers physically admixed to the polymer than for the respective polymeric UV absorbers. MA-TZ 1 embedded in poly(methyl methacrylate) shows an equal increase of phosphorescence intensity with UV irradiation time as the decrease of the proton-transferred fluorescence. By combining fluorescence and phosphorescence measurements it becomes possible to estimate the proportion of UV stabilizer molecules with an intermolecular hydrogen-bridge to poly(methyl methacrylate) and which are not suitable for light protection of polymers at room temperature. At low pressure and temperature, the increase of light-induced phosphorescence was delayed. This "phosphorescence induction" phenomenon can be put down to the free volume of polymer matrixes, in which various UV absorbers have been incorporated. The emission spectroscopic results are applicable to products which are customary in trade, as shown by investigations on a clear coat binder system.

1. Introduction

Intramolecularly hydrogen-bridged UV absorbers, such as 2-(2-hydroxyaryl)benzotriazoles (HBzTs) or 2-(2-hydroxyphenyl)-4,6-diaryl-1,3,5-triazines (HPTs), are widely used in polymer materials.[1−32] All of these compounds have one characteristic in common: an *excited state intramolecular proton transfer* (ESIPT) in the excited singlet state S_1 opens a pathway for the transformation of harmful ultraviolet radiation into thermal energy. In the case of HPTs, this was first investigated for the 2-hydroxyphenyl-1,3,5-triazines (see Scheme 1) in the pioneering work of Shizuka et al.[10a−f] Fundamental contributions to charge transfer in the excited state in general and the subsequent deactivation of excited hydrogen-bonded complexes have been made by Mataga and his group.[33−37] It has also been well established[38] that the chemical characteristic of an additive itself is not alone the decisive factor for assessing the effectiveness of light protection. Furthermore, physical loss of small stabilizer molecules also plays an important role.[38] Migration of UV absorber molecules out of the polymer is influenced by the free volume of the polymer as well as by the size and shape of the diffusing molecules.[39] To avoid pathways by which UV absorbers may be lost, polymerizable stabilizers[17,40−58] can be used, which are built directly into the polymer backbone via radical polymerization.

This paper reports on the copolymerization of MA-TIN 1 and MA-TZ 1 (see Chart 1) with styrene and methyl methacrylate (MMA) concerning the determination of copolymerization parameters. The emission spectroscopic behavior of these copolymers, compared with that of stabilizers simply admixed to the polymer, was investigated. Here the main emphasis was put on the influence of the polymer matrix and its thermodynamic properties. Thus, with the aid of a clear coat binder system, the question to be resolved was whether it is useful, from the viewpoint of application, to employ polymerizable UV stabilizers, which are more expensive, or only to physically admix the stabilizer with the polymer.

2. Experimental Section

2.1. Chemicals. The following compounds were synthesized by Ciba Specialty Chemicals, Inc., (Basle, Switzerland): MA-TIN 1, 2-[2-hydroxy-3-*tert*-butyl-5-(O-[2-hydroxy-3-(2-methylpropenoyloxy)-propyl]-2-carbonyloxyethyl)phenyl]benzotriazole; MA-TZ 1, 2,4-bis(2,4-dimethylphenyl)-6-[2-hydroxy-4-(2-hydroxy-3-[2-methylpropenoyloxy])propoxyphenyl]-1,3,5-triazine; D-OH-X, 2,4-bis(2,4-dimethylphenyl)-6-(2-hydroxy-4-dodecyloxyphenyl)-1,3,5-triazine; TTZ 3, 2,4-bis(2,4-dimethoxyphenyl)-6-(2-hydroxy-4-methoxyphenyl)-1,3,5-triazine; M-OH-P, 2,4-diphenyl-6-(2-hydroxy-4-methoxyphenyl)-1,3,5-triazine. MA-TIN 1 was recrystallized from hexane, MA-TZ 1

† Part of the special issue "Noboru Mataga Festschrift".

* To whom correspondence should be addressed. Fax: 0049-711-685-4495.

‡ Institut für Physikalische Chemie, Universität Stuttgart

§ Present address: PPG Industries Lacke GmbH, Talstr. 14, D-74379 Ingersheim, Germany.

|| Present address: GMI, Lisztweg 1, D-65812 Bad Soden, Germany.

⊥ Present address: DLR Institute of Technical Physics, Pfaffenwaldring 38-40, D-70569 Stuttgart, Germany.

3. Physikalisches Institut, Universität Stuttgart

▽ Ciba Specialty Chemicals Inc.

○ Present address: Vigier Cement AG, CH-2603 Péry, Switzerland.

10.1021/jp012134k CCC: $22.00
Published on Web 10/16/2001

SCHEME 1: Extended Otterstedt Scheme[5] for the Interpretation of Emission-Spectroscopic Results: 1. Absorption of the Closed Form; 2. Excited State Proton Transfer Enol → Keto; 3. Proton-Transferred Fluorescence; 4. Ground State Proton Transfer Keto → Enol; 5. Opening of the Intramolecular Hydrogen Bridge in the Ground State; 6. Relaxation Open → Closed Form with k_{rel}; 7. Absorption of the Open Form; 8. Intersystem Crossing of the Open Form; 9. Phosphorescence of the Open Form; 10. Radiationless Deactivation Process of the Excited Keto Form (Closed Form)

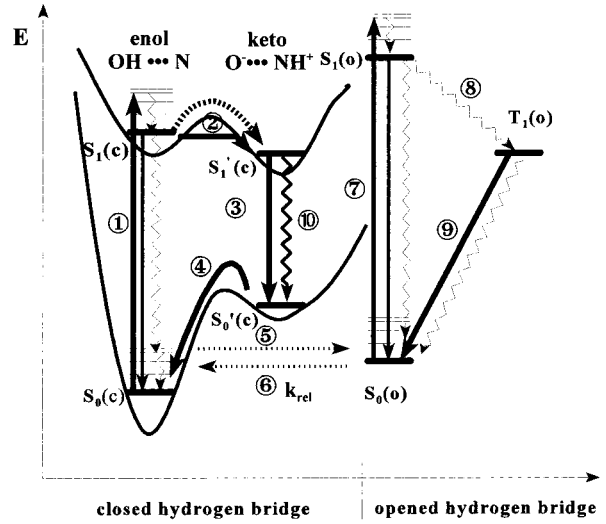

was recrystallized from methanol/water, TTZ 3 was recrystallized from toluene, and D-OH-X and M-OH-P were recrystallized first from anhydrous benzene and then from anhydrous toluene. Styrene was washed with 5% aqueous sodium hydroxide solution and with water. After drying over sodium sulfate, this styrene was distilled twice in a nitrogen atmosphere under reduced pressure over calcium hydride. Methyl methacrylate (MMA) was distilled twice at about 75 mbar over calcium hydride immediately before use. Butyl acrylate, butyl methacrylate, and 2-hydroxyethyl acrylate were distilled in vacuo over calcium hydride. The radical initiators AIBN (2,2′ azobisisobutyronitrile; 98%, Aldrich), and *tert*-butylperoxybenzoate (98%, Lancaster) were used without further purification.

Solvents. Toluene (anhydrous, Aldrich), 1,4-dioxane (Merck), acetone (Merck), and ethyl acetate (Aldrich) were spectroscopic grade. Solvents employed for copolymerization (i.e., toluene, *n*-hexane, and methanol) were purified by standard procedures.[59,60] Ethyl cellulose (Fluka) was used as supplied.

2.2. Synthesis of the Copolymers. *1. Styrene Copolymers.* To pure MA-TIN 1, or MA-TZ 1 dissolved in 5 mL of toluene (for the amounts of the UV absorbers see Tables 1 and 2) were added styrene (0.25−2.0 mL) and AIBN (15−20 mmol/L) dissolved in 5 mL of toluene. After degassing the polymerization mixtures by two freeze−pump−thaw cycles under nitrogen, the polymerization tubes were sealed at 3×10^{-2} mbar and placed in a constant-temperature bath at 70 °C for 30 min at the longest, so that the conversion did not exceed 5%. The crude copolymers were obtained by spray precipitation of the reaction mixtures into *n*-hexane, further purified by repeated dissolving/precipitation processes (toluene/*n*-hexane) until no more monomeric residue could be detected by gel permeation chromatography. The products were dried in vacuo (2×10^{-3} mbar) at 40 °C for at least 10 days.

2. Methyl Methacrylate Copolymers. The monomeric stabilizer (for the amounts of the UV absorbers; see Tables 1 and 2) was dissolved in methyl methacrylate (0.2−2.0 mL; MA-TZ 1 in additional 5 mL of toluene), AIBN was added (7.5−32 mmol/

CHART 1: Formulas and Designations

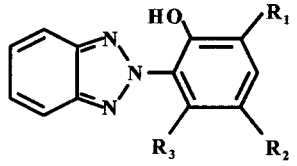

HBzT

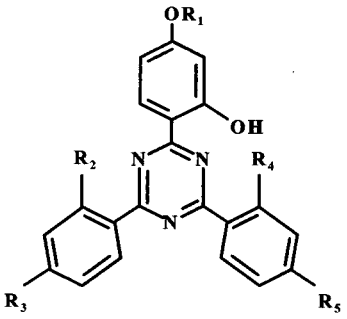

HPT

Compound	R_1	R_2	R_3	R_4	R_5
HBzT					
MA-TIN 1	$(CH_3)_3$	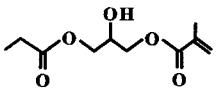	H	—	—
HPT					
MA-TZ 1	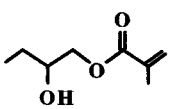	CH_3	CH_3	CH_3	CH_3
D-OH-X	*n*-$C_{12}H_{25}$	CH_3	CH_3	CH_3	CH_3
M-OH-P	CH_3	H	H	H	H
TTZ 3	CH_3	OCH_3	OCH_3	OCH_3	OCH_3

TABLE 1: Copolymerization of MA-TIN 1 with MMA and Styrene

monomer (M_2)	mmol MA-TIN 1 in monomer feed (M_1)	mole fraction of MA-TIN 1 in monomer feed (M_1)	conversion control (%)	mole fraction of MA-TIN 1 in copolymer
MMA	0.98	0.0494	2.7	0.0878
	0.46	0.1086		0.1761
	1.16	0.1099	3.4	0.1842
	0.41	0.1259		0.1981
	1.38	0.1632	5.4	0.2573
	0.64	0.2542		0.3490
styrene	1.29	0.0090		0.2023
	1.55	0.1058		0.2318
	0.55	0.1115	4.1	0.2289
	0.65	0.1292	4.5	0.2682
	1.35	0.1343		0.2815
	0.78	0.1513	3.2	0.2986
	0.44	0.1561		0.3035
	0.57	0.2061		0.3859

TABLE 2: Copolymerization of MA-TZ 1 with MMA and Styrene

monomer (M_2)	mmol MA-TZ 1 in monomer feed (M_1)	mole fraction of MA-TZ 1 in monomer feed (M_1)	conversion control (%)	mole fraction of MA-TZ 1 in copolymer
MMA	0.05	0.0056		0.0132
	0.08	0.0085	8.9	0.0192
	0.31	0.0319	5.3	0.0649
	0.52	0.0522	7.5	0.1121
	1.03	0.0990		0.2012
	0.48	0.1130	5.1	0.2102
	0.44	0.1326	8.6	0.2449
	0.44	0.1571	7.5	0.2663
styrene	0.93	0.0505		0.1559
	1.06	0.0747		0.2012
	0.90	0.0932		0.2341
	0.34	0.1355		0.3221
	0.70	0.1382	3.9	0.3221
	0.40	0.1557	5.4	0.3569

L), and after two freeze−pump−thaw cycles, the polymerization was allowed to proceed for approximately 15 min at 70 °C, so that the conversion did not exceed 10%. The precipitation and further purification process was the same as described above.

3. *Clear Coat Binder (CB).* [According to ref 61] Solution A: 8.4 mL (7.5 g; 58.5 mmol) of butyl acrylate, 9.1 mL (8.1 g; 57.0 mmol) of butyl methacrylate, 8.1 mL (9.0 g; 77.5 mmol) of 2-hydroxyethyl acrylate, 5.0 mL (4.5 g; 43.2 mmol) of styrene, 0.9 mL (0.9 g; 15.0 mmol) of glacial acetic acid, and 1.9 mL (2.0 g; 10.3 mmol) of *tert*-butyl peroxybenzoate. Solution B: 1.06 g (1.95 mmol) of MA-TZ 1, 20.0 mL toluene. An oven-dried 250 mL three-necked round-bottom flask fitted with a mechanical stirrer, reflux condenser with fixed nitrogen inlet, two 50 mL pressure-equalizing dropping funnels, and an internal thermometer was charged with 50 mL of dry toluene. The dropping funnels were filled with the solutions A and B (see above). Toluene was heated to 110 °C by means of an oil bath, and within 1 h, the solutions were added simultaneously dropwise to this stirred solvent. The reaction mixture was then stirred at about 110 °C for an additional 2 h under reflux. A total of 50 mL were removed from the mixture and precipitated from 350 mL of *n*-hexane (crude product CBI); the rest of the solution was stirred for another hour and then also precipitated from *n*-hexane (crude product CBII). The unstabilized polymers were obtained in the same manner, except that MA-TZ 1 was not included in solution B (crude products CBIII and CBIV). The crude products CB I−IV were purified by precipitation from toluene with *n*-hexane.

2.3. Measurements. *1. Absorption Spectra*. Absorption spectra were recorded with a Perkin-Elmer Lambda 7 UV/VIS absorption spectrometer.

2. Emission Spectra. All corrected spectra at various temperatures were measured on a built-in-house spectrometer described previously.[11,15,20] A 100 W high-pressure mercury lamp was employed as the excitation source. Fluorescence spectra of thin film samples were recorded using a front-face illumination geometry. These thin film samples of the copolymers were manufactured by spreading the polymers, dissolved in ethyl acetate/toluene-mixtures, onto quartz plates. After evaporation of the solvent, the films were dried in vacuo (2×10^{-3} mbar) at 40 °C for at least 10 days.

3. Gel Permeation Chromatography. The spectra were recorded on a gel permeation chromatograph Merck-Hitachi L-6000/L4250/D2520. The column was filled with PL-gel, and tetrahydrofurane (HPLC grade) was employed as solvent.

4. Elemental Nitrogen Analyses. Elemental nitrogen analyses were performed at the Institut für Organische Chemie, Universität Stuttgart, Germany.

5. Time-Resolved Fluorescence. Time-resolved fluorescence measurements were performed at the 3. Physikalisches Institut, Universität Stuttgart, Germany, using time-correlated single-photon counting after laser-pulse excitation (366 nm) by a synchronously pumped, cavity-dumped, and frequency-doubled dye laser. Corrections for light intensities and the spectral response of the apparatus were made.

3. Results and Discussion

3.1. Determination of Copolymerization Parameters. Various copolymers of MA-TIN 1 and MA-TZ 1 with styrene and methyl methacrylate (MMA) have been synthesized by radical polymerization. Although copolymers based on the compounds mentioned above have already been prepared, [31] these reactions have not yet been studied with respect to the determination of copolymerization parameters. Thus, for all four possible combinations of monomers, MA-TIN 1−styrene, MA-TIN 1−MMA, MA-TZ 1−styrene, and MA-TZ 1−MMA, the copolymerization parameters were determined. Because the solubility of MA-TIN 1 and MA-TZ 1 in styrene and MMA is not sufficient to obtain high mole fractions of UV stabilizer in the copolymer, the copolymerization of these monomeric UV stabilizers with styrene and MMA was carried out in toluene as solvent. This is also advantageous with regard to practical application, where normally solvents such as toluene or xylene[61] are employed. The composition of the copolymers was obtained from elemental nitrogen analysis, and UV/vis-spectroscopy and is shown as a function of the feed composition in Tables 1 and 2.

The conversion of the polymerization reaction did not exceed 6% for styrene copolymers and 10% in the case of MMA copolymers. The copolymerization parameters were obtained using functions of monomer feed composition vs composition of the copolymers, according to the Kelen−Tüdős(KT)[62] and the Yezrielev−Brokhina−Roskin(YBR) methods[63] (Table 3). The values of these copolymerization parameters constitute the ratio of addition rates of a monomer (i.e., MA-TIN 1) and a comonomer (i.e., styrene) to the propagating radical of the monomer (i.e., PMA-TIN 1). These investigations revealed that both examined UV absorbers were present to a higher extent in the copolymer than they are when simply present as mixture of monomeric UV absorbers in monomers MMA or styrene (see Figure 1).

TABLE 3: Calculated Copolymerization Parameters, Square of the Linear Correlation Coefficient (KT-method) and Sum of Least Squares (YBR-method)

	Kelen−Tüdős				Yezrielev−Brokhina−Roskin					
copolymer	r_{St}	r_{MMA}	$r_{MA-TIN1}$	r_{MA-TZ1}	r_{St}	r_{MMA}	$r_{MA-TIN1}$	r_{MA-TZ1}	R^2	$\Sigma(\Delta^2)$
PBS[a]	0.37		1.82		0.37		1.86		0.96	0.027
PBM[b]		0.52	1.10			0.52	1.14		0.99	0.018
PTS[c]	0.27			1.79	0.27			1.79	0.97	0.034
PTM[d]		0.43		1.35		0.43		1.39	1.00	0.182

[a] Poly[MA-TIN 1-*co*-(styrene)]; B ≡ "benzotriazole". [b] Poly[MA-TIN 1-*co*-(methyl methacrylate)]. [c] Poly[MA-TZ 1-*co*-(styrene)]; T ≡ "triazine". [d] Poly[MA-TZ 1-*co*-(methyl methacrylate)].

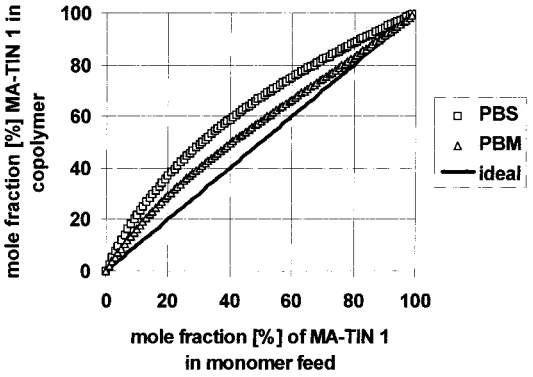

Figure 1. Copolymerization curves calculated from copolymerization parameters of the hydrogen-bridged benzotriazole MA-TIN 1 in poly-[MA-TIN 1-*co*-(styrene)] (PBS) and poly[MA-TIN 1-*co*-(methyl methacrylate)] (PBM).

3.2. Proton-Transferred Fluorescence. The temperature dependence of the proton-transferred fluorescence of MA-TIN 1- and MA-TZ 1-based copolymers has already been investigated by Keck et al.[31] For all copolymers from MA-TZ 1 and MA-TIN 1 with MMA and styrene investigated there, the correlation coefficients for the linear regression of the Arrhenius relationship in eq 1 were higher than 0.99;[31] here, Φ is the overall quantum yield of the proton-transferred fluorescence (see Scheme 1, parts 3 and 10), and E_a is the activation energy of the radiationless deactivation process:

$$\ln[\Phi(T_0)/\Phi(T) - 1] = -E_a/(RT) + C \qquad (1)$$

the constant C depends on the fluorescence lifetime at a temperature T_0, which is low enough that all radiationless processes may be assumed as frozen (here 77 K); $\tau(T_0)$ is the fluorescence lifetime at T_0, and A is the Arrhenius constant (eq 2):

$$C = \ln[A\tau(T_0)] \qquad (2)$$

For both MA-TZ 1 and MA-TIN 1, whether in monomeric or polymeric state, values for E_a of 4−5 kJ/mol and for C of 2−4 over a temperature range of 77−300 K are reported,[31] but in ref 31, as far as MA-TIN 1 and MA-TZ 1 physically admixed to a polymer matrix are concerned, nothing is said about the quality of the linear regression of eq 1 in distinguished temperature ranges, especially at room temperature or above, which are suitable for application. Therefore, for the model system MA-TIN 1/polystyrene, several temperature-dependent fluorescence spectra were recorded. The measurements covered a content of 10−74 wt % MA-TIN 1 in the mixtures and copolymers, respectively.

As an example, Figure 2a portrays the temperature dependence of the emission spectra (λ_{exc} = 366 nm) of the proton-transferred fluorescence of MA-TIN 1 (74 wt %) admixed to polystyrene, and Figure 2b portrays the Arrhenius plot according

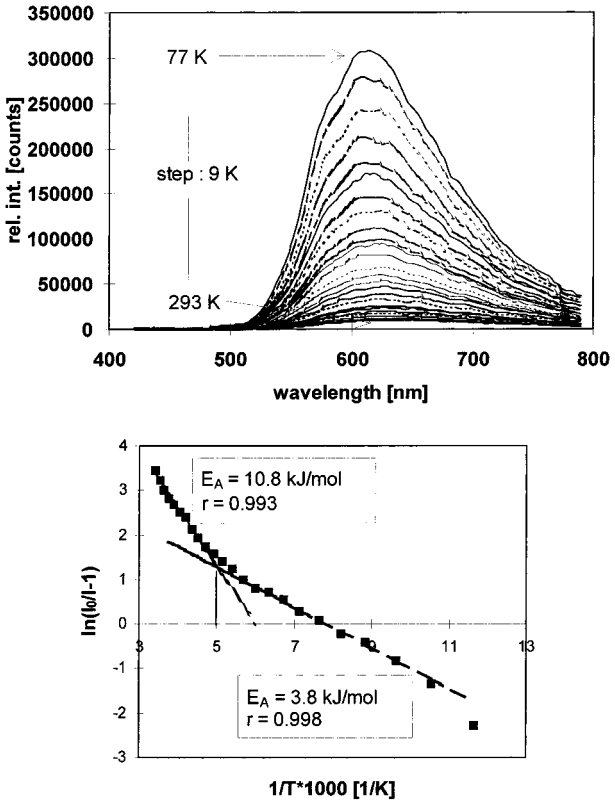

Figure 2. (a) Temperature dependence of the proton-transferred fluorescence (λ_{exc} = 366 nm) of a solid film of MA-TIN 1 (74 wt %) admixed to polystyrene (26 wt %) and (b) corresponding Arrhenius plot from the area under the emission curves in the wavelength region of 580 nm ≤ λ ≤ 680 nm, according to eq 1 (I ∼ Φ).

to eq 1 affiliated to these emission spectra. From Figure 2b, it immediately becomes apparent that this mixture exhibits a distinct high- and low-temperature behavior. At temperatures above 200 K, the calculated activation energy for the radiationless deactivation of the $S_1'(c)$ level amounts to 10.8 kJ/mol, whereas the calculation of the activation energy of the deactivation process below 170 K yields 3.8 kJ/mol. Between 200 and 170 K, there is a transition region, in which the high-temperature activation energy turns into the low-temperature energy. The Pearson coefficient for linear regression of eq 1 is higher than 0.99 for each of the separate temperature regions but not for the whole temperature range between 77 and 300 K. The intersection region of both regression lines lies between 212 and 173 K. On the basis of Figure 3, it can be visualized that the occurrence of the two different temperature ranges is not a function of the MA-TIN 1 concentration in a polystyrene matrix. With the same figure, it can also be shown that copolymers do not exhibit any deviation from an exact Arrhenius behavior and thus possess only one activation energy. All of the calculated data for activation energies E_a and the constant C for MA-TIN 1 in polystyrene are listed in Table 4.

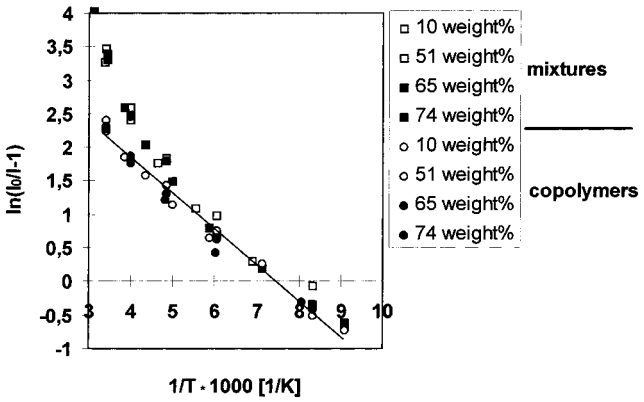

Figure 3. Comparison of the Arrhenius behavior between poly[MA-TIN 1-*co*-(styrene)] (circles) and mixtures of MA-TIN 1 and polystyrene (rectangles) with different ratios of MA-TIN 1 and polystyrene contents. The corresponding measurements of the proton-transferred fluorescence were carried out at $\lambda_{exc} = 366$ nm; the data were calculated from the area under the fluorescence curves in the wavelength region of 580 nm $\leq \lambda \leq$ 680 nm, according to eq 1.

A similar high- and low-temperature behavior for the photophysical properties of guest molecules in polymer matrixes was discovered by Guillet et al.[67a,68] When investigating temperature-dependent phosphorescence of doped polystyrene samples, they always found deviations from the linear Arrhenius behavior at a temperature of 180 ± 10 K, actually independent of the kind of guest molecule. Guillet and collaborators attributed these deviations to the transition temperature T_γ, at which in polymer matrixes side chain segment motions are frozen upon cooling the polymer sample. In the case of polystyrene, thermal freezing of the phenyl groups starts between 190 and 170 K. This result was also observed by other spectroscopic methods, like fluorecence spectroscopy [67b] and pulse radiolysis,[67c] and is in good agreement with those found in this work. The fact that normally no effect on the Arrhenius behavior of fluorescence at T_γ is observable is no contradiction to our measurements because usually the side chain segment motions cannot take place if the lifetime is very short.[68] In the case of polystyrene with admixed MA-TIN 1 where the proton-transferred singlet state has lifetimes longer than 100 ps (see Table 5 and ref 31) at 77 K, the local segmental motions in the polymer chain, which are certainly faster than 1×10^9 s^{-1},[69] possibly occur within the same time domain as the fluorescence decay time. Therefore, the polystyrene molecules can relax during the lifetime of the excited singlet state. Furthermore, from this, it can be concluded that MA-TIN 1 or similar molecules can serve as fluorescent probes for the determination of the transition temperature T_γ of polymers. This may be useful if other methods, such as differential scanning calorimetry, fail.

The activation energies E_a of the radiationless deactivation below T_γ are without exception significantly lower than the activation energies calculated for the same substance above T_γ. From this, it may be concluded that two different deactivation processes exist. If the chosen temperature is high enough, i.e., at room temperature or above, the faster deactivation process with the higher activation energy, involving sub-group motions in the polymer, becomes predominant. Opposite behavior is observed for the corresponding poly[MA-TIN 1-*co*-(styrene)] copolymers. They show an ideal Arrhenius behavior over the whole temperature range from 77 to 300 K in agreement with observations made by Keck et al.[31] The determined activation energies, however, are in the same order as those in the low-temperature area of the mixtures. It seems reasonable to interpret this as a consequence of steric requirements of the MA-TIN 1 molecules fixed into the polymer chain which makes segmental motions at the neighbor structure units more difficult; they are still frozen at room temperature. So, for the application of MA-TIN 1 as a UV absorber, MA-TIN 1 physically admixed to polystyrene becomes more and more favorable as the temperature is increased.

Generally, investigations of the proton-transferred fluorescence with MA-TZ 1 in a PMMA matrix give qualitatively the

TABLE 4: Calculated Activation Energies (for the System MA-TIN 1/PS) of Radiationless Deactivation E_a of the S_1'(c) State, the Parameter *C*, and Pearson Coefficients *r* for Linear Regression Lines in Different Temperature Regions

substance	morphology	wt % MA-TIN 1	parameters (Ea: [kJ/mol])	$T > 200$ K	$T < 170$ K	77 K $\leq T \leq$ 300 K
poly[MA-TIN 1-*co*-(styrene)]	powder	10	E_a			4.76
			C			4.24
			r			>0.99
MA-TIN 1/PS	powder	10	E_a	12.35	3.86	5.72
			C	8.53	3.79	5.43
			r			0.97
poly[MA-TIN 1-*co*-(styrene)]	powder	51	E_a			4.18
			C			3.79
			r			>0.99
MA-TIN 1/PS	powder	51	E_a	11.51	3.65	5.49
			C	7.94	3.32	5.05
			r			0.97
MA-TIN 1/PS	film	51	E_a	12.08	5.13	5.26
			C	9.08	4.66	4.97
			r			0.97
poly[MA-TIN 1-*co*-(styrene)]	powder	65	E_a			4.57
			C			4.07
			r			>0.99
MA-TIN 1/PS	powder	65	E_a	12.18	3.85	6.01
			C	8.23	3.51	5.44
			r			0.98
poly[MA-TIN 1-*co*-(styrene)]	powder	74	E_a			4.58
			C			3.98
			r			0.99
MA-TIN 1/PS	powder	74	E_a	10.75	3.78	5.25
			C	7.75	3.56	4.97
			r			0.96

TABLE 5: Lifetimes for MA-TIN 1 Fluorescence at about $\lambda_{obs} = 665$ nm

	mixture		copolymer			
temp [K]	τ_a' [ps]	τ_b' [ps]	τ_c' [ps]	τ_d' [ps]	τ_e' [ns]	τ_f' [ns]
296	27	60	9	19	2.13	0
230	38	103	12	71	1.35	8.3
210	48	145	13	99	1.20	7.9
200	56	164	14	139	1.26	9.1
190	66	174	16	168	1.23	32
170	75	230	17	203	1.4	37
140	80	280	22	214	1.4	27
120	90	320	30	244	1.38	13
77	117	450	50	276	1.38	12

same results as described for MA-TIN 1 in polystyrene. In this paper, they will not be discussed.

3.3. Dynamic Phosphorescence Phenomena. In a recent publication,[64] we established that in polar matrixes the phosphorescence intensity increases (with the shape of a $(1 - e)$ growth curve) when irradiating HPTs and HBzTs (each with an intramolecular hydrogen bond) with UV light, until an equilibrium value is reached.

This phosphorescence (step 9, Scheme 1) originates from a triplet state of the photoexcited open conformer (part III, Scheme 2) with an intermolecular hydrogen bridge, after the light-induced conversion from the "closed" form (I) to the "open" form (III) has taken place (step 5, Scheme 1). The conversion of an intramolecular to an intermolecular hydrogen bridge has been shown for TIN P (for detailed information see refs 11, 22, 23, 70, and 71), M-OH-P, and other HPTs (see Chart 1). For the latter, a kinetic model for the change in concentration of the open and closed form under photoexcitation has been evaluated.[64] Another scheme for the explanation of the photophysical behavior of compounds with an intramolecular hydrogen bridge was suggested by Catalán et al.[72] They have postulated that the photophysical behavior of TIN P and related compounds is determined by aggregates, such as dimers, and is not a consequence of an excited-state intramolecular proton transfer (ESIPT). We have discussed this aspect in an earlier publication;[32] moreover, the following results are compatible with a mechanism based on an ESIPT. There is no need to introduce dimers, or even more complex aggregates, to make the results explainable.

As opposed to samples kept at 77 K for several hours (Figure 4), the phosphorescence intensity of samples quenched from room temperature to 77 or 120 K does not rise quickly upon irradiation; it rather decreases at the beginning of UV irradiation (Figure 5). These results can only be interpreted by assuming the following two equilibria between the closed form (I) of MA-TZ 1 and the open form (III):

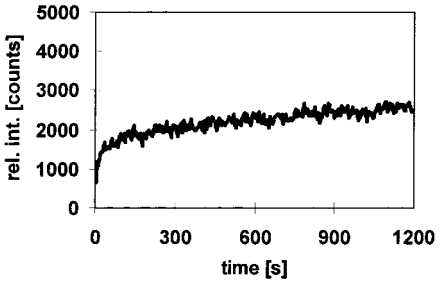

Figure 4. Phosphorescence evolution of a powdered sample of poly-[MA-TZ 1-*co*-(MMA)] (10 wt % MA-TZ 1) kept at 77 K for several hours ($\lambda_{exc} = 313$ nm, $\lambda_{obs} = 440$ nm, $T = 77$ K, pressure $= p_{77K} = 1 \times 10^{-3}$ mbar (N_2)). The ratio of intensity of the excitation light source is about 70:1 for the wavelengths of 366 and 313 nm. At $\lambda_{exc} = 366$ nm, only the closed form absorbs; thus, no phosphorescence is observable.

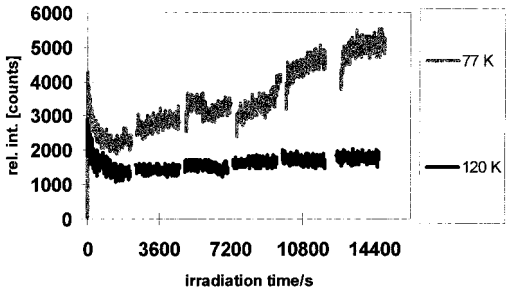

Figure 5. Phosphorescence evolution of two film samples of poly-[MA-TZ 1-*co*-(MMA)] (14 wt % MA-TZ 1) quick-frozen from room temperature to 77 and 120 K, respectively, ($\lambda_{exc} = 313$ nm and $\lambda_{obs} = 435$ nm).

(i) *Without irradiation* an equilibrium which depends only on temperature. As the "open" form has the higher energy (Scheme 1), the equilibrium is shifted to the *"closed" form (I)* when the temperature decreases, see eq 3:

$$\text{"closed" (I)} \rightleftharpoons \text{"open" (III)} \tag{3}$$

(ii) *Under irradiation* an equilibrium which causes an increase of phosphorescence intensity with prolonged UV irradiation (Figure 4). This equilibrium depends on both absorbed intensity I_{abs} and temperature because $k_{relaxation}$ (Scheme 1) decreases with

SCHEME 2: Different Structural Formulas of MA-TZ 1. (I) "Closed" Form, (II) Proton-Transferred "Closed" Form, Both with Intramolecular Hydrogen Bridge; (III) "Open" Form with Intermolecular Hydrogen Bridge.

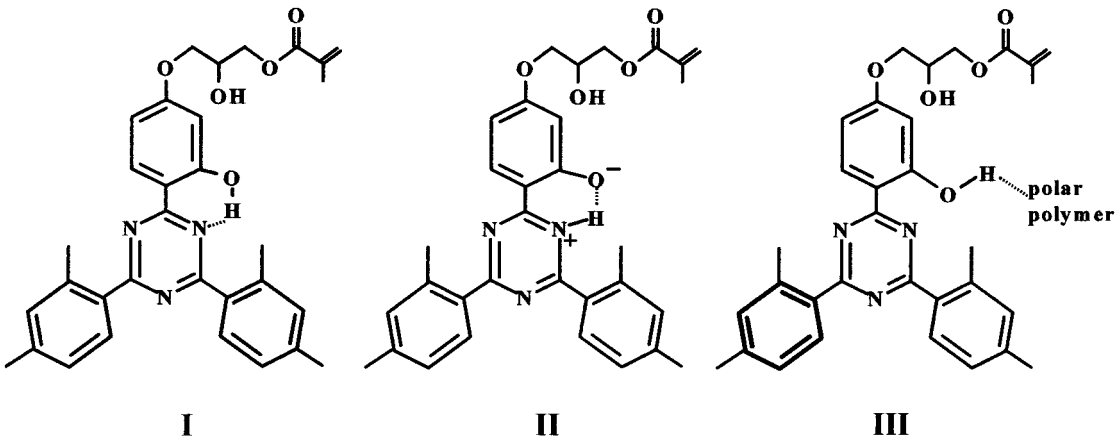

I II III

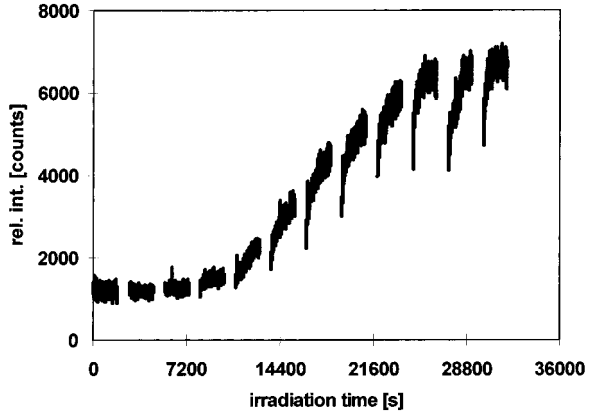

Figure 6. Phosphorescence induction shown by a powdered copolymer poly[MA-TZ 1-*co*-(MMA)] (10 wt % MA-TZ 1); $\lambda_{exc} = 313$ nm, $\lambda_{obs} = 440$ nm, pressure $= p_{292K} = 1 \times 10^{-3}$ mbar (N_2), then cooled to $T = 77$ K.

decreasing temperature. Thus, the equilibrium is shifted to the open form (III):

$$\text{“closed”(I)} \rightharpoonup \underset{k_{relaxation}}{\overset{I_{abs}}{\rightleftharpoons}} \rightharpoonup \text{“open”(III)} \qquad (4)$$

When samples are cooled rapidly to 77 K, the equilibrium according to eq 3 at room temperature with a higher amount of the open form is conserved. Therefore, upon immediate irradiation, a higher phosphorescence intensity arises (Figure 5) until the final lower equilibrium value (eq 3) of the open form corresponding to the lower temperature has been reached. This decrease is superimposed by the equilibrium according to eq 4. Establishing of this new equilibrium, causes an increase of phosphorescence.

With these two equilibria, however, it does not seem possible to explain the phosphorescence behavior of poly[MA-TZ 1-*co*-(MMA)] film samples at 77 K (Figure 6). This is due to a new phosphorescence phenomenon, henceforth designated phosphorescence induction, which is described in the following section.

Phosphorescence Induction. When exposing films of MA-TZ 1, either copolymerized with MMA or physically admixed to MMA, the phosphorescence of these film samples sometimes does not increase at the very beginning of UV irradiation. Only after a certain irradiation time has elapsed (see Figure 6; for poly[MA-TZ 1-*co*-(MMA)] containing 10 wt % MA-TZ 1, this time interval lasts about 3 h) then phosphorescence increases, because enough UV light energy is absorbed by the UV absorber molecules and transformed into thermal energy thus enabling them to come into contact with the polymer and to produce the open (phosphorescent) form. Also, relaxation (i.e., the regeneration of the “closed” form (I) when interrupting the UV irradiation) is observable as it is described more detailed in our last paper.[64] Our matter of concern was to elucidate this phenomenon, meaningful with respect to the light stabilization of polymers, by investigations concerning the influence of pressure, intensity, and duration of light exposure, as well as temperature and the matrix environment on the shape of the resulting phosphorescence intensity curves.

Because of the very complex nature of both the side-chain influences of MA-TZ 1 and the varnish binder system synthesized from various monomers, it was useful to investigate simpler and better-known systems, such as M-OH-P and D-OH-X in ethyl cellulose. Figure 7 portrays the changes in the phosphorescence behavior of M-OH-P in ethyl cellulose

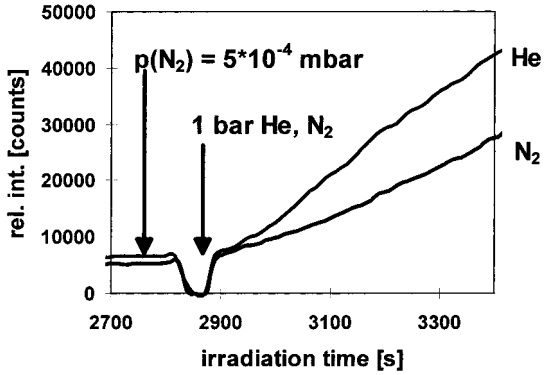

Figure 7. Two measurements to elucidate the pressure-dependent phosphorescence behavior of M-OH-P embedded in ethyl cellulose films; $\lambda_{exc} = 313$ nm, $\lambda_{obs} = 450$ nm, $p_{79K} = 5 \times 10^{-4}$ mbar (N_2), $T = 79$ K; during the measurements, the pressure is increased up to 1 bar of helium, or nitrogen, respectively.

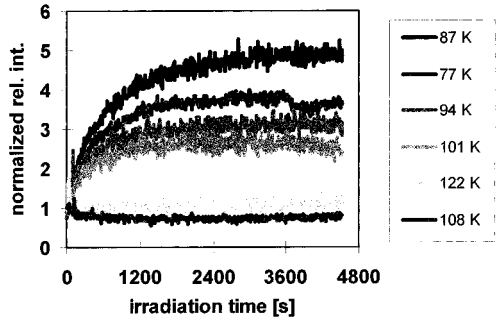

Figure 8. Change of the shape of phosphorescence evolution curves of poly[MA-TZ 1-*co*-(MMA)] films (14 wt % MA-TZ 1) with increasing temperature; $\lambda_{exc} = 313$ nm, $\lambda_{obs} = 440$ nm, $p = 1000$ mbar (N_2).

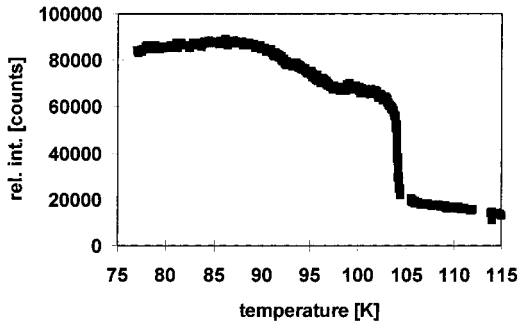

Figure 9. Temperature dependence of the phosphorescence of D-OH-X admixed to an ethyl cellulose film with increasing temperature; $\lambda_{exc} = 313$ nm, $\lambda_{obs} = 450$ nm, $p = 1000$ mbar (N_2). The irradiation dependent equilibrium (eq 4) is established.

starting from the induction period observable even until ca. 45 min after the beginning of irradiation and followed by the phosphorescence evolution period. The rise of gas pressure, either nitrogen or helium, from 5×10^{-4} to 1000 mbar triggers phosphorescence evolution within seconds.

The temperature dependence of the phosphorescence induction is shown in Figures 8 and 9. According to Figure 8, the highest temperature which allows observation of phosphorescence evolution is between 101 and 108 K for poly[MA-TZ 1-*co*-(MMA)] films under a constant nitrogen pressure of 1000 mbar in the cryostate. An exact determination of this transition temperature at the same nitrogen pressure was carried out with D-OH-X in an ethyl cellulose film (Figure 9). From Figure 9 ,it becomes immediately apparent that the phosphorescence of a preirradiated film decreases rapidly (until the two equilibria

SCHEME 3: Different Types of Volume in Polymer Chemistry in Dependence on Temperature.[65,66] V_f, Free Volume; $V_{unrelaxed}$, Entropic Unrelaxed Volume of the Polymer; V_0, Volume Extrapolated to $T = 0$ K; V_{spec}, Specific Polymer Volume; T_α, Glass Temperature; T_γ, Transition Temperature at Which the Side Chain Motions Become Frozen.

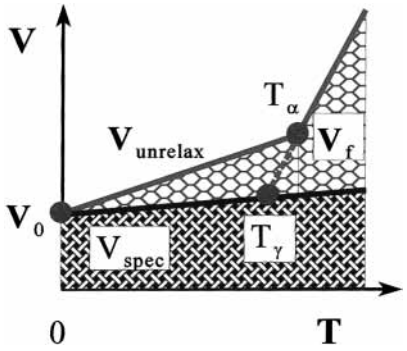

mentioned above are established) when heating the sample up to temperatures above 103 K. It is not possible to explain this result using the irradiation-dependent (eq 4) and the temperature-dependent equilibria (eq 3) alone.

Additionally, the transition from phosphorescence induction to phosphorescence evolution is shifted toward lower temperatures upon reduction of the nitrogen pressure around the sample holder. Finally, with a nitrogen pressure of 1×10^{-3} mbar, this transition is below 77 K, and right at the beginning of UV irradiation, phosphorescence induction is observed, whereas at 1 atm nitrogen pressure at 77 K, phosphorescence evolution occurs (Figure 8).

The influence of the temperature shown in Figures 8 and 9 as well as the results depicted in Figure 7 can be explained by the unrelaxed volume theory, vide infra.

This unrelaxed volume (see Scheme 3) is based on entropic effects.[65,66] The lower the temperature is, the more rigid the matrix is, which also decreases the rate of nonradiative decay processes. The possibility for the UV stabilizer to diffuse into this unrelaxed volume is reduced at lower temperatures. This also strengthens the contact between UV absorber and the hydrogen-bridge-accepting polymer matrix. When the temperature is low enough, the interaction of the UV absorber with the matrix becomes so strong that under irradiation with UV light the intramolecular hydrogen bond is converted to an intermolecular one. Thus, phosphorescence evolution can be observed.

The pressure-dependent emission measurements also support the suggestion that the unrelaxed volume is responsible for the time dependence of phosphorescence. When M-OH-P-films are evacuated at room temperature or a temperature not far below, the gas molecules (usually nitrogen was chosen) diffuse rapidly out of the polymer. When, in contrast to that, the film samples are first cooled to 77 K and then the films are evacuated, the gas molecules can only diffuse very slowly out of the polymer because of the small unrelaxed volume. So, still larger amounts of gas remain in the polymer films and occupy part of the volume which otherwise would be available for the incorporated M-OH-P molecules.

The available unrelaxed volume is much smaller in the films evacuated at 77 K than for the films evacuated at room temperature. Therefore, the contact of M-OH-P with ethyl cellulose is much better, and thus, phosphorescence evolution occurs (see Figure 10) even at very low nitrogen pressures. In comparison with that, the free volume of the polymer in the

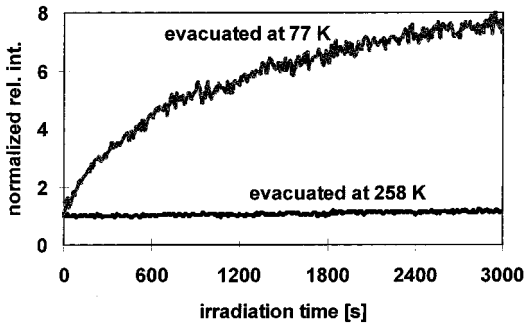

Figure 10. Dependence of phosphorescence evolution on the temperature, which was adjusted when evacuating film samples of 1.6 wt % M-OH-P in ethyl cellulose to $p = 1 \times 10^{-6}$ mbar (N_2); $\lambda_{exc} = 313$ nm, $\lambda_{obs} = 450$ nm, $T_{obs} = 77$ K.

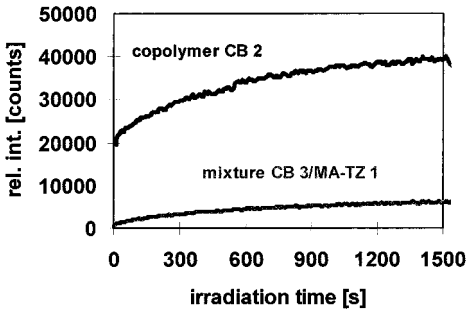

Figure 11. Light-induced phosphorescence evolution in a clear coat binder with copolymerized MA-TZ 1 as well as in a mixture of unstabilized binder and MA-TZ 1. Both investigated substances contain 6 wt % MA-TZ 1; $\lambda_{exc} = 313$ nm, $\lambda_{obs} = 440$ nm, $T_{obs} = 77$ K.

samples degassed ($p = 1 \times 10^{-3}$ mbar) at higher temperatures is large enough to allow diffusion of M-OH-P into the holes of the ethyl cellulose matrix. Even when the sample is cooled to 77 K, there hardly exists any contact between the UV stabilizer molecules and the ethyl cellulose matrix; that is, the intramolecular hydrogen bonds remain intact. Consequently, phosphorescence induction is observable.

If, however, a sample, which shows phosphorescence induction, is treated with nitrogen or helium (see Figure 7), the gas occupies free space in the surface layers of the polymer because of the enormous pressure gradient (5×10^{-4} mbar inside the sample/1000 mbar surrounding the sample). Thus, the available unrelaxed volume decreases immediately, the UV stabilizer molecules come into contact with the polar polymer, the intramolecular hydrogen bridge is opened, and phosphorescence evolution occurs.

3.4. Copolymer or Mixture? As described in section 3.2, there are some indications that for practical application at room temperature and above UV stabilizers are more suitable for light protection, if they are admixed instead of copolymerized. To answer the question definitely, whether the use of copolymers or mixtures is more advantageous, it appears reasonable to have a closer look at the population of the long-living triplet state T_1(o) of the open form (see Scheme 2, part III, and Scheme 1) caused by the opening of the intramolecular hydrogen bridge by UV irradiation. From this triplet state, several degradation reactions can start. Figure 11 clearly shows that phosphorescence evolution occurs with both MA-TZ 1 copolymerized and admixed to the varnish binder. However, with copolymerized MA-TZ 1, the phosphorescence intensity at the very beginning of UV irradiation is not zero. Moreover the phosphorescence intensity is higher for copolymers than for MA-TZ 1 admixed to unstabilized binder at any time during irradiation. That means that in the case of binder copolymers the more open form of

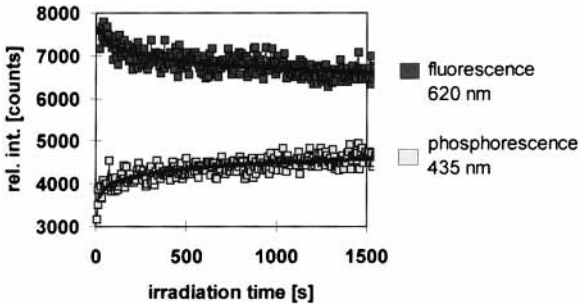

Figure 12. Irradiation time dependent fluorescence and phosphorescence of p[MA-TZ 1-*co*-(MMA)] with 14.1 wt % incorporated MA-TZ 1; $\lambda_{exc} = 313$ nm, $T = 77$ K.

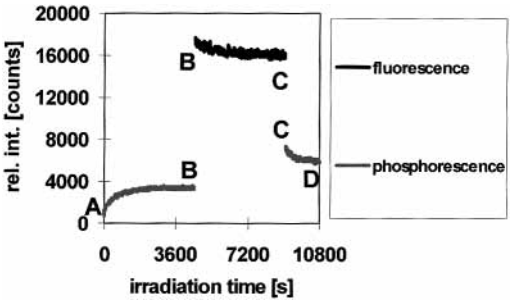

Figure 13. Combined measurement of the fluorescence ($\lambda_{exc} = 366$ nm and $\lambda_F = 620$ nm) and the phosphorescence ($\lambda_{exc} = 313$ nm and $\lambda_P = 440$ nm) of a copolymer from MA-TZ 1 and MMA with 7.9 wt % MA-TZ 1; $T = 91$ K. At $\lambda_{exc} = 366$ nm, only the closed form absorbs (see ref 64); thus, no phosphorescence is observable. For A−D, see the text.

UV stabilizer is created and, therefore, the triplet-state population via process 8 in Scheme 1 is increased compared with mixtures. This is also explainable with the given free volume model, because in the copolymer the MA-TZ 1 structure units are fixed on the polymer chain and are not able to diffuse into holes of the polymer. It seems that the interaction of the UV absorber with an hydrogen attracting polymer matrix such as PMMA is stronger in the copolymer than in the mixture, because of a closer arrangement, and therefore, more open conformers of MA-TZ 1 result. Thus, the photophysical behavior is more favorable in mixtures than in copolymers.

For the decision whether a substance is suitable for light protection, it is important to know how many of the UV absorber molecules possess an intermolecular hydrogen bond at room temperature. Unfortunately, the phosphorescence emission is not directly observable at room temperature, due to rapid radiationless processes of the triplet state. It is possible, however, to shock-freeze samples to 77 K within a few seconds and to get in this way further information concerning the state of the system at room temperature. From Figure 5, it becomes apparent that after irradiating a shock-frozen poly[MA-TZ 1-*co*-(MMA)]-sample (14 wt % MA-TZ 1) for several hours the same order of phosphorescence intensity is reached as at the very first beginning of irradiation (at $T = 77$ K). That means approximately the same amount of MA-TZ 1 molecules are opened at 77 K as in the nonirradiated MA-TZ 1 at room temperature, because the room-temperature state of eq 3 still remains conserved when shock-freezing the sample rapidly to 77 K. If it were possible to calculate how many molecules are opened due to the irradiation-dependent equilibrium at 77 K, the question would also be answered for room temperature. Fortunately, Figure 12 illustrates that an increase of phosphorescence (due to the generation of the "opened" form of the molecules; step 5, Scheme 1) goes along with a decrease of proton-transferred fluorescence. This PTF stems from those molecules, whose intramolecular hydrogen bond is still intact. Thus, those molecules phosphoresce which cannot participate in the Förster cycle (steps 1−4, Scheme 1).[73,74] As mentioned before, mixtures held several hours at 77 K before UV irradiation do not show any phosphorescence. Therefore, combined fluorescence and phosphorescence measurements at 77 K have to be carried out to estimate the amount of open form at room temperature. In Figure 13, such a measurement is portrayed. Under irradiation ($\lambda_{exc} = 313$ nm), MA-TZ 1 (7.9 wt % in PMMA) shows phosphorescence evolution in the transition from A to B. When the excitation wavelength is changed to $\lambda_{exc} = 366$ nm, fluorescence is observed. Only the closed form is excited in this case (in ref 64 it is shown that a noteworthy absorption of the "open" form of the M-OH-P triazine type only exists at wavelengths below $\lambda_{abs} = 350$ nm), and because of the opening of intramolecular hydrogen bridges (step 5 in Scheme 1), the fluorescence decreases from time B to C during irradiation. Upon irradiating the sample again with light of the wavelength $\lambda_{exc} = 313$ nm, the phosphorescence changes until at time D the irradiation-dependent equilibrium (eq 4) is finally established. The decrease of phosphorescence from C to D is due to the different number of light quanta absorbed per time unit by MA-TZ 1 at both different excitation wavelengths (see also legend to Figure 4). From the measurements portrayed in Figure 13, the ratio of closed-to-opened form of 83:17 at 77 K was calculated.[76] In combination with Figure 5, it may be concluded that at room temperature there are never more than 17% of the stabilizer molecules in the open form. On the basis of earlier measurements with TTZ 3 which possesses a strong intramolecular hydrogen bridge[31,75] (stronger than that of MA-TZ 1), a closed-to-open-form ratio of 92:8 was calculated[76] (for a detailed depiction of the somewhat lengthy calculations of the closed-to-open ratio see ref 76, pp 129−136). Because of the very rapid relaxation process (step 6, Scheme 1) at room temperature this value is not exceeded even under UV irradiation (eq 4). Thus, UV stabilizers such as MA-TZ 1 are good UV protecting substances, because the temperature-dependent equilibrium (equation 4) is shifted far to the closed form at room temperature which is favorable for protection against light.

3.5. Time-Resolved Fluorescence Spectroscopy. To describe the decay profiles (see Figure 14) of MA-TIN 1 admixed to polystyrene properly, a biexponential fit is required. τ_b' is the main component with the longer lifetime (see Table 5).

Figure 15 illustrates that from data analysis of the longer lifetime τ_b' high- and low-temperature behavior of MA-TIN 1/polystyrene mixtures can also be derived, though E_a and C derived from time-resolved measurements have somewhat smaller values than those obtained by determination from steady-state fluorescence.

For the copolymer, the decay curves are nonexponential, and a corresponding analysis is more difficult. For a proper fit, four time constants are needed, two shorter ones (τ_c' and τ_d') in the picosecond time range and two longer ones (τ_e' and τ_f') in the nanosecond time range. The resulting decay constants can only be regarded as average lifetimes, whereas the contributions of the two shorter time constants (τ_c' and τ_d') are predominant. Comparing the decay dynamics of mixture and copolymer it can be stated that the lifetimes of the excited proton-transferred state of MA-TIN 1 in the powdered mixture (τ_a' and τ_b') are longer than the dominating lifetimes of the copolymer.

This can be related to the different molecular packing in both forms. In the case of the mixture MA-TIN 1 is microcrystalline,

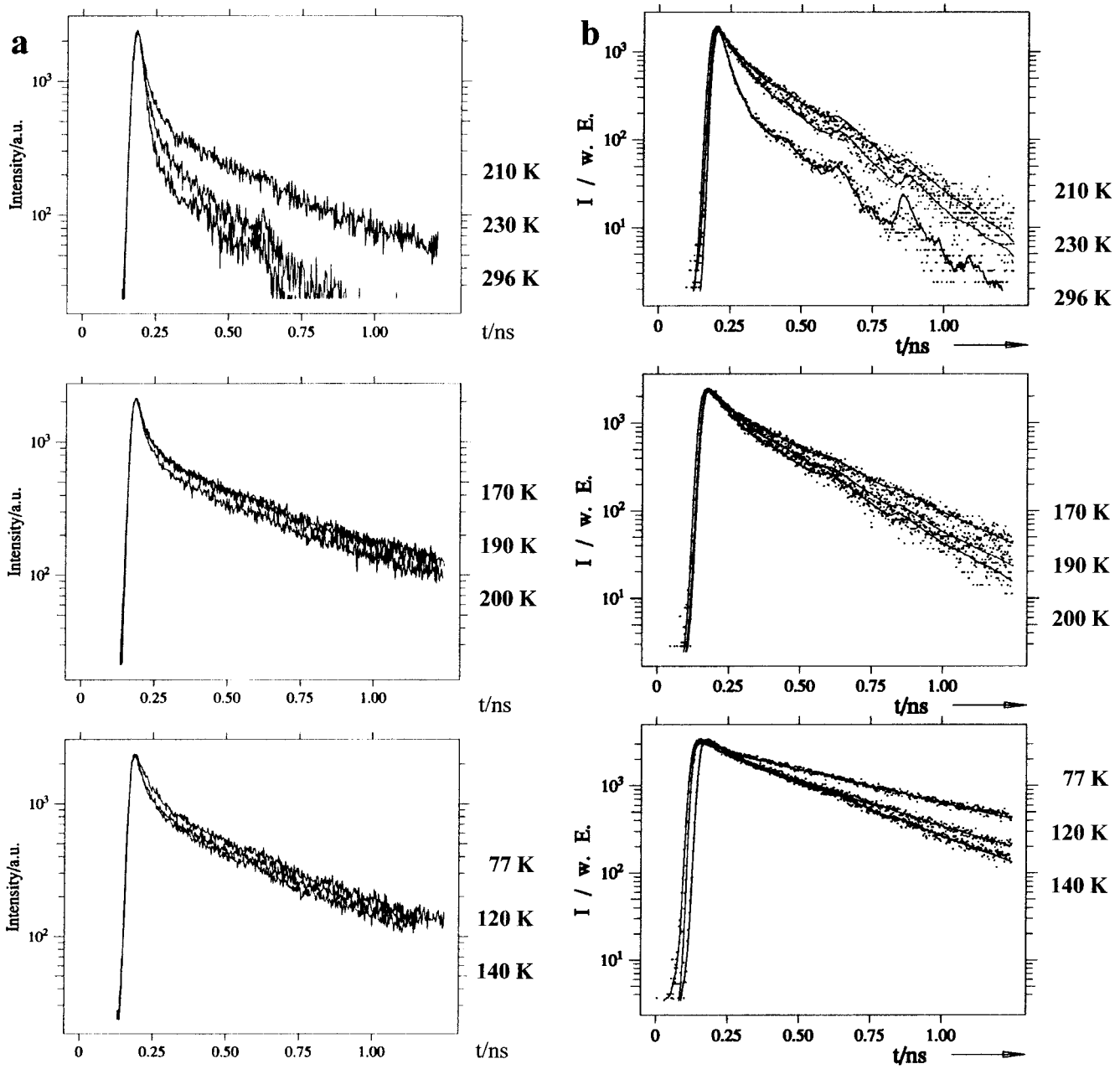

Figure 14. Fluorescence decay profiles (λ_{exc} = 363 nm and λ_{obs} = 667 nm) of (a) the copolymer p[MA-TIN 1-*co*-(styrene)] (10 wt % MA-TIN 1) and (b) 10 wt % MA-TIN 1 admixed to polystyrene at various temperatures.

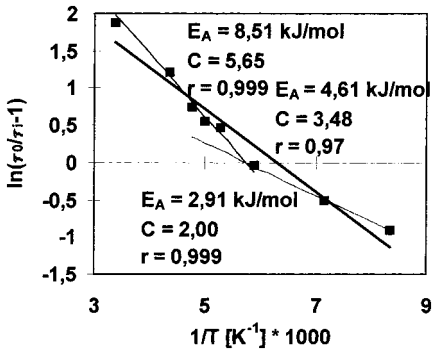

Figure 15. Arrhenius plot for the mixture MA-TIN 1 (10 wt %)/polystyrene generated from time-resolved fluorescence measurements by analysis of τ_b'. The Pearson coefficient of the high- and low-temperature range is derived from the correlation lines marked in.

so the molecules are packed closer than in the copolymer.[31] This is the reason for the longer lifetimes in the mixtures. It may be assumed that the short lifetime is, due to the enhanced amorphous structure, more representative than the longer one. From steady-state measurements, it may be concluded that an Arrhenius plot provides very good correlation coefficients for the copolymer. These are indeed also obtainable from time-resolved fluorescence measurements, as becomes apparent from Figure 16.

The maximum of the observed PTF of copolymers is red-shifted in comparison to mixtures. From this, it may be concluded that the coiled structure of copolymers forces the UV stabilizer molecules out of planarity, and this means that the energy difference between S_1'(c) and the S_0'(c) state (see Scheme 1) decreases.

4. Conclusions

The copolymerization parameters of both copolymerizable UV absorbers investigated, MA-TIN 1 and MA-TZ 1, are larger than 1. On the other hand, the copolymerization parameters for

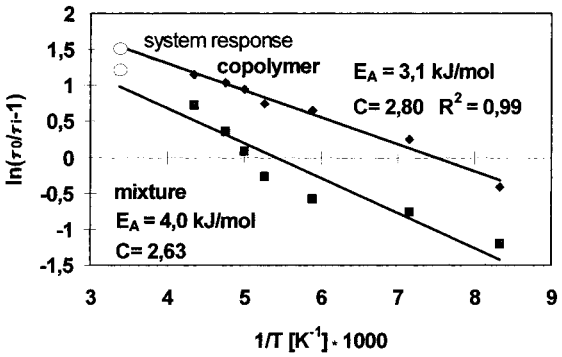

Figure 16. Comparison between short lifetimes in a powdered mixture (τ_a') and a powdered copolymer sample (τ_c') for the system MA-TIN 1 (10 wt %)/ polystyrene.

the comonomers styrene and methyl methacrylate are smaller than 1. On the basis of the copolymerization parameters obtained, it turned out that in each of the examined copolymerization systems the UV stabilizer was present to a higher extent than it was when simply present as a mixture of monomeric UV absorbers in the monomer feed.

Measurements of the proton-transferred fluorescence (PTF) were utilized to analyze the efficiency of the radiationless deactivation from the S_1'(c) level (Scheme 1). On the basis of the results from these investigations (and of course especially from those outlined in section 3.4) the conclusion was drawn that radiationless deactivation (step 10 in Scheme 1) is more efficient in copolymers than in mixtures at temperatures far below 200 K. In mixtures, however, these deactivation steps are clearly more efficient than in copolymers *at room temperature* or above.

From Arrhenius plots, it became apparent that for copolymers a linear relation was obtained in any case, in contrast to the mixtures. This is also confirmed by time-resolved fluorescence measurements. Mixtures show a distinguishable high- and low-temperature behavior due to the freezing of motions in the side-chains of the polymer matrix at a transition temperature T_γ dependent on the chosen polymer matrix.

Both MA-TZ 1 in the copolymerized state as well as physically admixed to a hydrogen attracting polymer matrix show phosphorescence evolution when irradiating samples with radiation (λ_{exc} = 313 nm) from an 100 W Hg-arc lamp. The observed intensity of this emission assumes the shape of a (1 − e) growth curve in dependence on irradiation time.

From the photophysical point of view alone, it would not be necessary to synthesize the more costly copolymers, because they exhibit phosphorescence at the very beginning of irradiation, whereas the phosphorescence intensity of the corresponding mixtures starts from zero. Additionally, at room temperature, the radiationless deactivation is less favored in copolymers than in mixtures. However, in copolymers the UV stabilizer cannot migrate out when covalently fixed to the polymer backbone which might favor copolymers for long-term use.

The free-volume theory is suitable to determine whether phosphorescence evolution or the recently discovered delayed phosphorescence evolution phenomenon, the phosphorescence induction, is observable. Low pressures shift the light-induced equilibrium between the conformers with an intact intramolecular hydrogen bridge (closed form) and the open form with an intermolecular hydrogen bridge toward the closed form. The polymer matrix has a strong influence on the population of the triplet state via its unrelaxed volume and, therefore, for the suitability of a substance to protect a polymer against light degradation.

Because the equilibrium without irradiation between the open and the closed form (eq 3) even at room temperature is almost completely shifted to the closed form and relaxation, due to an equilibrium under irradiation (eq 4), from the open to the closed form is very fast, UV absorbers such as MA-TZ 1 are good light-protecting agents.

References and Notes

(1) Heller, H. J.; Blattmann, H. R. *Pure Appl. Chem.* **1972**, *30*, 145−165.
(2) Heller, H. J.; Blattmann, H. R. *Pure Appl. Chem.* **1973**, *36*, 141−161.
(3) Heller, H. J. *Eur. Polym. J.*—*Suppl.* **1969**, 105−132.
(4) Williams, D. L.; Heller, A. *J. Phys. Chem.* **1970**, *74*, 4473−4480.
(5) Otterstedt, J.-E. A. *J. Chem. Phys.* **1973**, *58*, 5716−5725.
(6) Werner, T.; Kramer, H. E. A.; Kuester, B.; Herlinger, H. *Angew. Makromol. Chem.* **1976**, *54*, 15−29.
(7) Kuester, B.; Tschang, Ch.-J.; Herlinger, H. *Angew. Makromol. Chem.* **1976**, *54*, 55−70.
(8) Werner, T.; Kramer, H. E. A. *Eur. Polym. J.* **1977**, *13*, 501−503.
(9) Kloepffer, W. In *Advances in Photochemistry*; Pitts, J. N., Jr., Hammond, G. S., Gollnick, K., Eds.; Wiley: New York, 1977; Vol. 10, pp 311−358.
(10) (a) Shizuka, H.; Matsui, K.; Okamura, T.; Tanaka, I. *J. Phys. Chem.* **1975**, *79*, 2731−2734. (b) Shizuka, H.; Matsui, K.; Hirata, Y.; Tanaka, I. *J. Phys. Chem.* **1976**, *80*, 2070−2072. (c) Shizuka, H.; Matsui, K.; Hirata, Y.; Tanaka, I. *J. Phys. Chem.* **1977**, *81*, 2243−2246. (d) Shizuka, H.; Machii, M.; Higaki, Y.; Tanaka, M.; Tanaka, I. *J. Phys. Chem.* **1985**, *89*, 320−326. (e) Moriyama, M.; Kaurakami, Y.; Tobita, S.; Shizuka, H. *Chem. Phys.* **1998**, *231*, 205−214. (f) Moriyama, M.; Kosuge, M.; Tobita, S.; Shizuka, H. *Chem. Phys.* **2000**, *253*, 91−103.
(11) Werner, T. *J. Phys. Chem.* **1979**, *83*, 320−325.
(12) Werner, T.; Woessner, G.; Kramer, H. E. A. *ACS Symp. Ser.* **1981**, *151*, 1−18.
(13) Huston, A. L.; Scott, G. W.; Gupta, A. *J. Chem. Phys.* **1982**, *76*, 4978−4985.
(14) Flom, S. R.; Barbara, P. F. *Chem. Phys. Lett.* **1983**, *94*, 488−493.
(15) Woessner, G.; Goeller, G.; Kollat, P.; Stezowski, J. J.; Hauser, M.; Klein, U. K. A.; Kramer, H. E. A. *J. Phys. Chem.* **1984**, *88*, 5544−5550.
(16) Woessner, G.; Goeller, G.; Rieker, J.; Hoier, H.; Stezowski, J. J.; Daltrozzo, E.; Neureiter, M.; Kramer, H. E. A. *J. Phys. Chem.* **1985**, *89*, 3629−3636.
(17) O'Connor, D. B.; Scott, G. W.; Coulter, D. R.; Gupta, A.; Webb, S. P.; Yeh, S. W.; Clark, J. H. *Chem. Phys. Lett.* **1985**, *121*, 417−422.
(18) Arnaut, L. G.; Formosinho, S. J. *J. Photochem. Photobiol. A: Chem.* **1996**, *100*, 15−34.
(19) Kramer, H. E. A. *Farbe + Lack* **1986**, *92*, 919−924.
(20) Goeller, G.; Rieker, J.; Maier, A.; Stezowski, J. J.; Daltrozzo, E.; Neureiter, M.; Port, H.; Wiechmann, M.; Kramer, H. E. A. *J. Phys. Chem.* **1988**, *92*, 1452−1458.
(21) Gormin, D.; Heldt, J.; Kasha, M. *J. Phys. Chem.* **1990**, *94*, 1185−1189.
(22) Kramer, H. E. A. In *Studies in Organic Chemistry 40: Photochromism—Molecules and Systems*; Duerr, H., Bouas-Laurent, H., Eds.; Elsevier: Amsterdam, 1990; pp 654−684.
(23) Kramer, H. E. A. In *Book of Abstracts, 13th Inernational Conference on Advances in the Stabilization and Degradation of Polymers*, Lucerne, Switzerland, May 22−24, 1991; Patsis, A. V., Ed.; The Institute of of Material Science, State University of New York: New Paltz, NY, 1991; pp 59−78.
(24) Catalán, J.; Jerez, P.; Fabero, F.; Wilshire, J. F.; Claramunt, R. M.; Elguero, J. *J. Am. Chem. Soc.* **1992**, *114*, 964−966.
(25) Catalán, J.; Del Valle, J.; Fabero, F.; Garcia, N. A. *J. Photochem. Photobiol.* **1995**, *61*, 118−123.
(26) Catalán, J.; de Paz, J. L. G.; Torres, M. R.; Tornero, J. D. *J. Chem. Soc., Faraday Trans.* **1997**, *93*, 1691−1699.
(27) Catalán, J.; Díaz, C. *J. Phys. Chem. A* **1998**, *102*, 323−328.
(28) Bigger, S. W.; Ghiggino, K. P.; Leaver, I. H.; Scully, A. D. *J. Photochem. Photobiol. A: Chem.* **1987**, *40*, 391−399.
(29) Stueber, G. J.; Kieninger, M.; Schettler, H.; Busch, W.; Goeller, B.; Franke, J.; Kramer, H. E. A.; Hoier, H.; Henkel, S.; Fischer, P.; Port, H.; Hirsch, T.; Rytz, G.; Birbaum, J.-L. *J. Phys. Chem.* **1995**, *99*, 10097−10109.
(30) Kieninger, M.; Scherf, H.; Stueber, G. J.; Roessler, M.; Fischer, P.; Schmidt, A.; Kramer, H. E. A. In *Book of Abstracts, 34th International IUPAC Symposium on Macromolecules*; Prague, July 13−18, 1992; Czechoslovak Chemical Society: Prague, 1992; Contribution No. 8, p 4.
(31) Keck, J.; Kramer, H. E. A.; Port, H.; Hirsch, T.; Fischer, P.; Rytz, G. *J. Phys. Chem.* **1996**, *100*, 14468−14475.

(32) Keck, J.; Roessler, M.; Schroeder, C.; Stueber, G. J.; Waiblinger, F.; Stein, M.; LeGourriérec, D.; Kramer, H. E. A.; Hoier, H.; Henkel, S.; Fischer, P.; Port, H.; Hirsch, T.; Rytz, G.; Hayoz, P. *J. Phys. Chem B* **1998**, *102*, 6975−6985.
(33) Okada, T.; Karaki, I.; Mataga, N. *J. Am. Chem. Soc.* **1982**, *104*, 7191−7195.
(34) Martin, M. M.; Ikeda, N.; Okada, T.; Mataga, N. *J. Phys. Chem.* **1982**, *86*, 4148−4156.
(35) Ikeda, N.; Miyasaka, H.; Okada, T.; Mataga, N. *J. Am. Chem. Soc.* **1983**, *105*, 5206−5211.
(36) Mataga, N. *Pure Appl. Chem.* **1984**, *56*, 1255−1268.
(37) Kakitani, T.; Matsuda, N.; Yoshimori, A.; Mataga, N. *Prog. React. Kinet.* **1995**, *20*, 347−381.
(38) Foeldes, E. *J. Appl. Polym. Sci.* **1993**, *48*, 1905−1913 and references therein.
(39) Foeldes, E. *Polym. Degr. Stab.* **1995**, *49*, 57−63.
(40) Decker, C.; Zahouily, K. *J. Polym. Sci: A: Polym. Chem.* **1998**, ***36***, 2571−2580.
(41) Plotnikov, V. G.; Efimov, A. A. *Russ. Chem. Rev.* **1990**, *59*, 792−806.
(42) Nir, Z.; Vogl, O.; Gupta, A. *J. Polym. Sci: Polym. Chem. Ed.* **1982**, *20*, 2735−2754.
(43) Rasoul, F. A.; Pasch, H.; Shuhaibar, K. F.; Attari, A. *Angew. Makromol. Chem.* **1991**, *193*, 159−167.
(44) Li, S.; Albertsson, A.-C.; Gupta, A.; Basset, W., Jr.; Vogl, O. *Monatsh. Chem.* **1984**, *115*, 853−868.
(45) Braun, D.; Most, D.; Ziser, T. *Angew. Makromol. Chem.* **1994**, *221*, 187−205.
(46) Braun, D.; Ghahary, R.; Ziser, T. *Angew. Makromol. Chem.* **1995**, *233*, 121−131.
(47) Sustic, A.; Zhang, C.; Vogl, O. *J. Mass Spectrom.—Pure Appl. Chem.* **1993**, *30*, 741−755.
(48) Shuhaibar, K. F.; Rasoul, F. A.; Pasch, H.; Mobasher, A. *Angew. Makromol. Chem.* **1991**, *193*, 147−158.
(49) Vogl, O.; Albertsson, A.-C.; Janovic, Z. *ACS Symp. Ser.* **1985**, *280*, 197−210.
(50) Li, T.; Li, S.; Fu, S.; Vogl, O. *J. Macromol. Sci.—Chem.* **1991**, *28*, 673−685.
(51) Vogl, O.; Albertsson, A.-C.; Janovic, Z. *Polymer* **1985**, *26*, 1288−1296.
(52) Borsig, E.; Kárpátyová, A.; Vogl, O. *Collect. Czech. Chem. Commun.* **1989**, *54*, 996−1004.
(53) Ruhlmann, D.; Zahouily, K.; Fouassier, J. P. *Eur. Polym. J.* **1992**, *28*, 1063−1067.
(54) O'Connor, D. B.; Scott, G. W.; Coulter, D. R.; Yavrouian, A. *J. Phys. Chem.* **1991**, *95*, 10252−10261.
(55) Tocker, S. *Makromol. Chem.* **1967**, *101*, 23−32.
(56) Menon, S. V.; Parmar, J. S. *Angew. Makromol. Chem.* **1993**, *210*, 61−68.
(57) Atkinson, D.; Lehrle, R. *Eur. Polym. J.* **1992**, *28*, 1569−1575.
(58) Konstantinova, T. *Angew. Makromol. Chem.* **1996**, *243*, 51−55.
(59) Perrin, D. D.; Armarego, W. L. F. *Purification of Laboratory Chemicals*; Pergamon Press: Oxford, U.K., 1988.
(60) Pestemer, M. *Anleitung zum Messen von Absorptionsspektren im Ultraviolett und Sichtbaren*; Georg Thieme Verlag: Stuttgart, Germany, 1964.
(61) EP 0 434 619 A2. Ciba-Geigy Ltd.
(62) Kelen, T.; Tüdős, F. *J. Macromol. Sci.—Chem.* **1975**, *9*, 1−27.
(63) Yezrielev, A. I.; Brokhina, E. L.; Roskin, Y. S. *Vysokomol. Soedin.* **1969**, *A11*, 1670−1680; In: *Chem. Abstr. 71*: 124981f.
(64) Waiblinger, F.; Keck, J.; Stein, M.; Fluegge, A. P.; Kramer, H. E. A.; Leppard, D. *J. Phys. Chem. A* **2000**, *104*, 1100−1106.
(65) Muruganandam, N.; Koros, W. J.; Paul, D. R. *J. Polym. Sci: B: Polym. Phys.* **1987**, *25*, 1999−2026.
(66) Puleo, A. C.; Muruganandam, N.; Paul, D. R. *J. Polym. Sci: B: Polym. Phys.* **1989**, *27*, 2385−2406.
(67) (a) Somersall, A. C.; Dan, E.; Guillet, J. E. *Macromolecules* **1974**, *7*, 233−244. (b) Smit, K. J.; Sakurovs, R.; Ghiggino, K. P. *Eur. Polym. J.* **1983**, *19*, 49−53. (c) Szadowska-Nicze, M.; Mayer, J. *J. Polym. Sci. A: Polym. Chem.* **1998**, *36*, 1209−1215.
(68) Guillet, J. E. *Pure Appl. Chem.* **1977**, *49*, 249−258.
(69) Tagawa, S.; Nakashima, N.; Yoshihara, K. *Macromolecules* **1984**, *17*, 1167−1169.
(70) Orton, E.; Morgan, M. A.; Pimentel, G. C. *J. Phys. Chem.* **1990**, *94*, 7936−7943.
(71) Yamaguchi, S.; Hirota, N. *J. Am. Chem. Soc.* **1988**, *110*, 1346−1351.
(72) Catalán, J.; Fabero, F.; Guijarro, M. S.; Claramunt, R. M.; Santa Maria, M. D.; de la Conception Foces-Foces, M.; Cano, F. H.; Elguero, J.; Sastre, R. J. *Am. Chem. Soc.* **1990**, *112*, 747−759.
(73) Förster, Th. *Z. Elektrochem.* **1950**, *54*, 42−46; 531−535.
(74) Weller, A. In *Progress of Reaction Kinetics*; Porter, G., Ed.; Pergamon: London, 1961; Vol. I, pp 187−214.
(75) Fischer, P.; Fettig, A. *Magnet. Reson. Chem.* **1997**, 35, 839−844.
(76) Stein, M. Ph.D. Thesis, Universität Stuttgart, Stuttgart, Germany, 1999.